Human Lysosomal β-Galactosidase−Cathepsin A Complex: Definition of the β-Galactosidase-Binding Interface on Cathepsin A†

Alexey V. Pshezhetsky, Marc-André Elsliger, Maya V. Vinogradova,‡ and Michel Potier*

Service de Génétique Médicale, Hôpital Sainte-Justine, Département de Pédiatrie, Université de Montréal, Montréal, Québec, Canada H3T 1C5

Received September 21, 1994; Revised Manuscript Received November 21, 1994®

ABSTRACT: Human lysosomal β-galactosidase is organized as a 680-kDa complex with cathepsin A (also named carboxypeptidase L and protective protein), which is necessary to protect β-galactosidase from intralysosomal proteolysis. To understand the molecular mechanism of β-galactosidase protection by cathepsin A, we defined the structural organization of their complex including the β-galactosidase-binding interface on cathepsin A. Radiation inactivation analysis suggested the existence of a 168-kDa structural subunit of the complex containing both β-galactosidase and cathepsin A. Chemical cross-linking of the complex confirmed the existence of this subunit and showed that it is composed of one cathepsin A dimer and one β-galactosidase monomer. The modeling of the cathepsin A dimer tertiary structure based on atomic coordinates of a wheat carboxypeptidase suggested a putative β-galactosidase-binding cavity formed by the association of two cathepsin A monomers. According to this model two exposed loops of cathepsin A bordering the cavity were chosen as part of a putative β-galactosidase-binding interface. Synthetic peptides corresponding to these loops were found both to dissociate the complex and to inhibit its *in vitro* reconstitution from purified cathepsin A and β-galactosidase. The defined location of the GAL monomer in the complex with 35% of its surface covered by the CathA dimer may explain the stabilizing effect of CathA on GAL in lysosome.

Soon after the concept of the lysosome was proposed, Koenig (1962) suggested that lysosomal enzymes may be protected against intralysosomal proteolytic digestion by association into supramolecular structures to form a lysosomal matrix. This concept has found some support at least in the case of β-galactosidase (GAL,[1] EC 3.2.1.23) and neuraminidase (NEUR, EC 3.2.1.18) from both genetic and physicochemical evidence. These two glycosidases are associated in the lysosome with cathepsin A (CathA, lysosomal carboxypeptidase, protective protein, EC 3.4.16.1) to form a high molecular weight complex essential for stabilization of GAL and NEUR (d'Azzo et al., 1982; Hoogeveen et al., 1983; Verheijen et al., 1985; Van der Horst et al., 1989). The functional importance of this supramolecular organization is confirmed by the existence of a human inherited disease, galactosialidosis, where CathA deficiency is responsible for the secondary loss of GAL and NEUR activities in patients' cells (Wenger et al., 1978; Suzuki et al., 1984; Palmeri et al., 1986; Galjart et al., 1988; Tranchemontagne et al., 1990). Recent homology modeling of the human CathA using the X-ray crystal structure of the wheat carboxypeptidase II (Liao et al., 1992) as template suggested that most mutations in galactosialidosis patients affect the stability of the CathA protein (Elsliger & Potier, 1994). The characterization of various galactosialidosis mutations in CathA (Zhou et al., 1991; Shimmoto et al., 1993) as well as site-directed mutagenesis studies of CathA active site residues (Galjart et al., 1991) established that the instability of GAL and NEUR in galactosialidosis results from the absence of their structural interactions with CathA.

To understand the molecular mechanism underlying the stabilization of GAL and NEUR by CathA, it is necessary to determine the structural organization of their complex. Previous work (Pshezhetsky & Potier, 1993) has shown that the majority of GAL in the lysosome is found in the 680-kDa complex containing four GAL and eight CathA protomers as the only components. NEUR activity is associated with a higher molecular mass complex of about 1280 kDa, also containing GAL and CathA. The total amount of GAL and CathA in the 1280-kDa complex purified from human placenta represents only about 1% of their amount found in the 680-kDa complex (Pshezhetsky & Potier, 1994).

In this paper, using both radiation inactivation and chemical cross-linking studies, we demonstrate that the 680-kDa complex is composed of four basic subunits each made of one GAL monomer and one CathA dimer. A structural model of the CathA dimer (Elsliger & Potier, 1994) is used to define a putative binding interface with GAL. Synthetic peptides corresponding to this region in the CathA model are tested *in vitro* for their capacity to (1) dissociate the purified GAL−CathA complex, (2) hamper the reassociation

† This work was supported in part by a Chercheur invité award from the Fonds de la recherche en santé du Québec to A.V.P. and by an operating grant from the Medical Research Council of Canada to M.P. A.V.P. and M.-A.E. contributed equally to this work as first authors.

* To whom correspondence should be addressed at the Service de Génétique Médicale, Hôpital Sainte-Justine, 3175 Côte Sainte-Catherine, Montréal, Québec, Canada H3T 1C5 [telephone (514) 345-4931,; Fax (514) 345-4801].

‡ Present address: A. N. Belozersky Institute of Physico-Chemical Biology, Moscow State University, Moscow, Russia 119899.

® Abstract published in *Advance ACS Abstracts,* January 15, 1995.

[1] Abbreviations: GAL, galactosidase; NEUR, neuraminidase; CathA, cathepsin A; Muf-β-Gal, 4-methylumbelliferyl β-D-galactopyranoside; CBZ-Phe-Leu, *N*-carbobenzoxy-L-phenylalaninyl-L-leucine; EDC, 1-ethyl-3-[3-(dimethylamino)propyl]carbodiimide; DMA, dimethyl adipimidate; DMS, dimethyl suberimidate; 3,3′-DSP, 3,3′-dithiobis(succinimidyl propionate); RIS, radiation inactivation size; TS, target size.

0006-2960/95/0434-2431$09.00/0

of CathA with GAL, and (3) bind to purified GAL. Two such synthetic peptides had all of these properties, allowing us to propose a structure for the GAL-binding interface on the CathA dimer.

EXPERIMENTAL PROCEDURES

Peptides. The synthetic peptides (PC-1, PC-2, and PC-3) derived from CathA were purchased from Bio-Synthesis, Inc. (Louisville, TX). They had the following sequences: PC-1, NH_2-V^{400}KYGDSGE^{407}-NH_2; PC-2, NH_2-Q^{76}PDGVTLEY^{84}-NH_2; and PC-3, NH_2-Y^{221}DNKDLECVT^{230}-NH_2. The peptides were more than 90% pure by HPLC and had the correct monoisotopic molecular masses determined by FAB−mass spectrometric analysis: PC-1, 854 Da; PC-2, 1021 Da; and PC-3, 1199 Da. The p*I* values of the peptides (PC-1, 6.1; PC-2, 4.1; PC-3, 3.8) were calculated with the MacBioSpec software (Perkin-Elmer, Thornhill, Ontario). Human angiotensin II (95% pure) was purchased from Sigma Chemical Co (St. Louis, MO).

Purification of the 680-kDa GAL−CathA Complex. The GAL−CathA complex was purified from human placenta as described by Pshezhetsky and Potier (1993) using affinity chromatography on concanavalin A−Sepharose and *p*-aminophenyl thio-β-D-galactopyranoside (PATGAL)−agarose, followed by FPLC gel filtration. The purified preparation was concentrated to 0.8 mg/mL and stored at 4 °C for up to 30 days without loss of GAL and CathA activities.

Dissociation of the Complex into GAL and CathA. The preparation of the GAL−CathA complex was dissociated by overnight dialysis against 10 mM Tris-HCl buffer, pH 7.5. CathA and GAL were separated by FPLC anion-exchange chromatography (Pshezhetsky & Potier, 1993). Purified preparations of CathA and GAL were dialyzed against 20 mM sodium acetate, pH 4.75, 0.15 M NaCl, and 0.02% (w/v) NaN_3 (buffer A) and concentrated approximately to 0.25 mg of protein/mL in Minicon concentration cells (Amicon).

Radiation Inactivation and Fragmentation Analysis. The purified enzyme preparations of the GAL−CathA complex (0.51 mg of protein/mL), CathA (0.33 mg/mL) and GAL (0.145 mg/mL), all in buffer A, were frozen in liquid nitrogen and kept at −80 °C until irradiated. The frozen samples were irradiated at −78 °C in a Gammacell Model 220 ^{60}Co source (Nordion International Inc., Kanata, Canada) with increasing doses of γ-rays (dose rate of about 1 Mrad/h; 100 rad is 1 Gy) as previously described by Beauregard et al. (1987). Irradiated samples were thawed at 4 °C and immediately analyzed for GAL and CathA activities. The samples were also analyzed for the remaining nondegraded protein (Beauregard et al., 1987) by FPLC gel filtration on a Superose 6 HR column and by SDS−PAGE (11% gel, w/v) under reducing conditions (Laemmli, 1970). Proteins were stained with Coomassie blue R-250 and quantitated by scanning with an Ultroscan XL laser densitometer (LKB). Appropriate controls of nonirradiated preparations were analyzed under the same conditions. The linearity of the microdensitometer response (up to 20 μg of protein loaded on the gel) was previously established. The densitometer peak areas were all corrected for variable bandwidths on the gel.

The radiation inactivation size (RIS, the mass of 1 mol of enzyme inactivated by a radiation hit) and the target size (TS, the mass of 1 mol of protein fragmented by a hit) were computed from the equation (Beauregard et al., 1987):

$$\log (\text{RIS or TS}) = 5.89 - \log D_{37,t} - 0.0028t \quad (1)$$

where t is the irradiation temperature in °C and $D_{37,t}$ is the radiation dose necessary to inactivate enzyme or to reduce the amount of protein to 37% of the initial value. $D_{37,t}$ values were calculated from a semilogarithmic decay plot of enzyme activity or of the remaining protein versus radiation dose.

Chemical Cross-Linking of the Complex Components. The GAL−CathA complex preparation (50 μL, 0.2 mg of protein/mL of buffer A) was incubated with 2.5 or 5 μL of freshly prepared solutions of the appropriate cross-linking reagent. The concentrations of the cross-linkers in the stock solutions were 2 mg/mL for 3,3′-dithiobis(succinimidyl propionate) (3,3'-DSP) in dimethyl sulfoxide or 20 mg/mL for dimethyl suberimidate (DMS), dimethyl adipimidate (DMA), and 1-ethyl-3-[3-(dimethylamino)propyl]carbodiimide (EDC) in water. A solution of 0.1 M $NaCO_3$ was used to adjust the pH of the reaction mixture up to the optimal values (pH 7.5 for 3,3′-DSP and EDC or pH 9.0 for DMS and DMA). The mixture was incubated at 25 °C for 1 h (Bragg & Hou, 1986), and 25 μL of 1.5 M Tris-HCl buffer, pH 6.8, was added to quench the cross-linking reaction. The sample was further incubated for 30 min at 25 °C and analyzed by SDS−PAGE on a 5−15% (w/v) polyacrylamide gradient gel (0.7-mm slab thickness) under nonreducing conditions according to Laemmli (1970). The proteins were stained by Coomassie blue R-250.

Analysis of the Cross-Linked Products. After the first electrophoresis (as described above) Coomassie blue-stained bands of cross-linked protomers were excised from the gel, incubated in the appropriate reaction medium to cleave the cross-linkers as described by Bragg and Hou (1986), and inserted into the wells of a stacking gel on the top of a 11% (w/v) polyacrylamide gel slab (1 mm thick). The second electrophoresis was run under reducing conditions. The gels were stained by combined Coomassie blue R-250 and silver staining using Fast Silver kit (Bio-Rad) and scanned using an Ultroscan XL laser densitometer (LKB). GAL and CathA protomers in each cross-linked product were quantitated using a calibration curve made with purified GAL and CathA (Pshezhetsky & Potier, 1993). The densitometer peak areas were all corrected for variable bandwidths on the gel.

Homology Modeling of the Cathepsin A Dimer. The molecular modeling of the CathA dimer was carried out as previously described (Elsliger & Potier, 1994) using the atomic coordinates of the wheat serine carboxypeptidase II (CPDW-II; Protein Data Bank file 3SC2) as template with the exception of the Thr^{210} to Thr^{230} loop region which was modeled on the coordinates of the corresponding loop in yeast serine carboxypeptidase Y (CPDY) since it can better accommodate the four-residue insertion not present in CPDW-II. The atomic coordinates of the CPDW-II dimer and of CPDY were kindly provided by Dr. S. J. Remington (University of Oregon, Eugene). Two previously identified N-linked glycosylation sites (Asn^{117} and Asn^{305}) were included in the model (Morreau et al., 1992). The solvent accessibility of residue side chains in the CathA dimer was computed using the DSSP program (Kabsch & Sander, 1983). Side chains with accessible surfaces greater than 30 Å^2 (approximating a 20% mean side-chain accessibility) were classified as solvent accessible. Peptide segments spanning

seven residues and containing at least five solvent-accessible residues were selected because of their potential capacity to interact with GAL. Peptides close to the active site pocket, glycosylation sites, or CathA dimerization interface were rejected. The remaining peptides were visualized on the CathA model with the QUANTA-CHARMM software (Molecular Simulations Inc., Burlington, MA) running on a Silicon Graphics Iris Indigo workstation (Mountain View, CA). The solvent-accessible dot surface of the proposed binding interface was generated with QUANTA-CHARMM using a probe radius of 1.4 Å according to Connolly (1983).

In Vitro Reconstitution and Dissociation of the GAL−CathA Complex. To evaluate the effect of CathA-derived synthetic peptides on the complex reassociation, purified preparations of CathA and GAL, each in buffer A, 0.25 mg/mL, were mixed in a CathA:GAL molar ratio of 2:1 in the presence of increasing amounts of peptides. The mixture was incubated at 37 °C for 60 min, and the relative amounts of reconstituted complex, GAL, and CathA were analyzed by FPLC gel filtration on a Superose 6 HR column eluted with buffer A.

To determine the effect of the peptides on the complex dissociation, a concentrated preparation of the GAL−CathA complex (0.8 mg of protein/mL) was diluted 1:2 by buffer A containing varying amounts of peptides or their mixture and incubated at 37 °C for 60 min. The samples were then analyzed by gel filtration as above. It was verified that the synthetic peptides had no effect on GAL and CathA specific activities under the experimental conditions used for the reconstitution and dissociation experiments.

Peptide Binding to GAL and the GAL−CathA Complex. The PC-1 Tyr residue was radiolabeled with ^{125}I using the Radioiodination Labeling kit of Du Pont (Wilmington, DE) according to the manufacturer's specifications. The specific radioactivity of the labeled peptide was 0.334 μCi/mg. Labeled PC-1 was incubated with the GAL−CathA complex in final concentrations of 0.65, 1.6, 2.6, and 3.25 mM. The incubation mixture was analyzed by gel filtration on a Superose 6 HR column as above, and the radioactivity was measured in eluted fractions. PC-1 binding to the complex or to individual GAL tetramers was analyzed by a Scatchard plot (Scatchard, 1949) according to the equation:

$$r/[\text{PC-1}] = -r/K_d + n/K_d \quad (2)$$

where

$$r = [\text{PC-1}_{bound}]/[\text{GAL}_{total}] \quad (3)$$

n is the number of PC-1 binding sites per mole of GAL, and K_d is the equilibrium dissociation constant of the GAL−PC-1 complex.

The PC-1 and CathA binding to GAL was also studied by their influence on the kinetic parameters of GAL using 4-methylumbelliferyl β-galactopyranoside (Muf-β-GAL) as substrate. The apparent Michaelis−Menten constant, K_m, was determined using 0.0625−1.25 mM substrate concentrations and 0.18 μg of purified GAL in buffer A at 37 °C in the presence of increasing concentrations of peptide or purified CathA.

Enzyme Assays. The GAL activity was assayed according to Okada and O'Brien (1968) with Muf-β-GAL as substrate and the CathA activity according to Tranchemontagne et al. (1990) with CBZ-Phe-Leu as substrate at 37 °C and pH 4.75. One unit of enzyme activity (U) is defined as the amount of enzyme that hydrolyzes 1 μmol of substrate/min. Proteins were assayed according to Bradford (1976) with bovine serum albumin as standard.

RESULTS

Radiation Inactivation. The radiation inactivation and fragmentation method of protein analysis is based on the target theory (Lea, 1955) which states that a single hit by an ionizing radiation on a protein will fragment its polypeptide chain and completely abolish the biological activity and that the probability of a protein to be hit is proportional to its molecular size. Therefore, protein M_r can be estimated (eq 1) by the analysis of the decay curves of the biological activity versus radiation dose (radiation inactivation size, RIS) or of the remaining nondegraded protein versus radiation dose (target size, TS). In the case of protein complexes or oligomeric proteins, TS and RIS usually correspond to the M_r of single protomers, but RIS values corresponding to several protomers or to whole oligomers have also been reported (Potier et al., 1991, 1994). In the latter case it has been suggested that either each protomer is required for the expression of the biological activity of the oligomer or that the radiation energy absorbed by one protomer is transferred to the other protomers inside the oligomer (Potier et al., 1991, 1994; Kempner & Fleisher, 1989).

Such energy transfer seems to take place in the case of the irradiation of the GAL−CathA complex. The TS values of GAL and CathA (Figure 1 and Table 1) corresponded approximately to the molecular masses of their protomers—64 and 52 kDa, respectively. The same TS values were calculated for both α and β protein chains of CathA, indicating that the destructive energy absorbed by the protein after a hit is transferred between the chains through disulfide bridges as previously demonstrated for ricin (Kempner & Fleisher, 1989).

In contrast, RIS of GAL and CathA were significantly higher than TS values (Figure 1 and Table 1). The close values obtained for the RIS of GAL (144 ± 16 kDa) and for that of CathA (167 ± 26 kDa) are consistent with a model where both GAL and CathA are inactivated by a single radiation hit inside the same subunit. Inside this substructure, the destructive energy absorbed in one GAL or CathA monomer is transferred to the other adjacent protomer(s), causing simultaneous inactivation of the two enzymes from a single hit.

However, the same experimental results could also be expected from energy transfer within homooligomers of GAL and CathA. In order to verify this, we performed radiation inactivation analysis of isolated CathA dimers and GAL tetramers. For both enzymes, RIS and TS values corresponded to the molecular masses of their corresponding protomers (Table 1), indicating that the destructive energy is not transferred between protomers of isolated CathA or GAL oligomers.

Chemical Cross-Linking Analysis. The structural arrangement of CathA and GAL protomers inside the complex was further studied by the chemical cross-linking method. SDS−PAGE analysis of the cross-linked products (Figure 2; letters between the brackets refer to bands on the gel) showed that

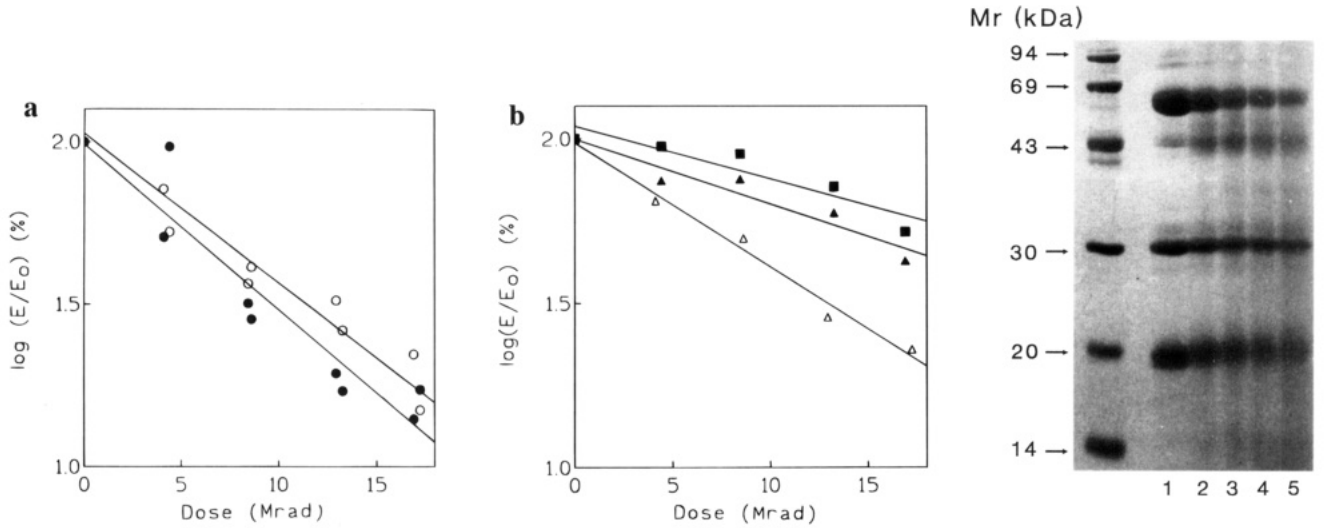

FIGURE 1: Radiation inactivation (a) and fragmentation (b) of GAL and CathA in the 680-kDa GAL−CathA complex at −78 °C. Irradiation was carried out in duplicate as described in Experimental Procedures. Irradiated samples were thawed at 4 °C and immediately assayed for GAL and CathA activities and analyzed by SDS−PAGE. The log percent of remaining GAL (○) activity and CathA (●) activity and the intensity of GAL (△), CathA α-chain (■), and CathA β-chain (▲) bands on the SDS gel are plotted as a function of radiation dose. Inset into panel b (right): SDS−PAGE analysis of the irradiated GAL−CathA complex on 11% (w/v) gel. Samples containing 20 μg of the complex were applied in each lane after irradiation with the following doses: unirradiated control, lane 1; 4.42 Mrad, lane 2; 8.45 Mrad, lane 3; 13.25 Mrad, lane 4; 16.9 Mrad, lane 5.

Table 1: Radiation Inactivation Size (RIS) and Target Size (TS) of GAL and CathA in Their Oligomeric Forms and in the 680-kDa GAL−CathA Complex[a]

preparation	assay method	RIS (kDa)	TS (kDa)
free form			
GAL (tetramer)	activity	63 ± 3 (3)	
	SDS−PAGE		68 ± 3 (3)
	FPLC		52 ± 4 (3)
CathA (dimer)	activity	64 ± 12 (3)	
	SDS−PAGE		
	α-chain		58 ± 14 (3)
	β-chain		44 ± 7 (3)
	FPLC		59 ± 15 (3)
complex			
protein[b]	FPLC		630 ± 50 (3)
GAL	activity	144 ± 12 (6)	
	SDS-PAGE		66 ± 5 (6)
CathA	activity	167 ± 26 (6)	
	SDS-PAGE:		
	α-chain		49 ± 4 (6)
	β-chain		56 ± 9 (6)

[a] The mean ± SE of three and more determinations is shown. The number of determinations is indicated in parentheses. [b] Analysis of the protein content of the the GAL−CathA complex peak eluted from the FPLC column.

3,3′-DSP, corresponding to a 1.1-nm bridge between Cys residues of the two proteins, cross-linked species with apparent molecular mass of 75 ± 20 [A], 138 ± 15 [B], 300 ± 20 [C], and 550−600 [E] kDa. DMS and DMA (1.1- and 0.9-nm bridges between amino groups of proteins, respectively) yielded the same major bands of 78 ± 20 [A], 150 ± 10 [B], 280 ± 20 [C], 380 ± 20 [D], and 550−600 [E] kDa, but the relative amounts of species with molecular mass of 280 ± 20 [C] and 380 ± 20 [D] kDa were much higher with DMS. EDC which makes 0.2-nm bridges between amino groups of proteins gave mostly 80 ± 10 [A] and 150 ± 10 [B] kDa products. Thus, there appears to be an increase in the mass of the cross-linked species with the length of cross-linker bridge, supporting the conclusion that these species exist in a complex. In addition, we did not observe any cross-linked products when the complex was

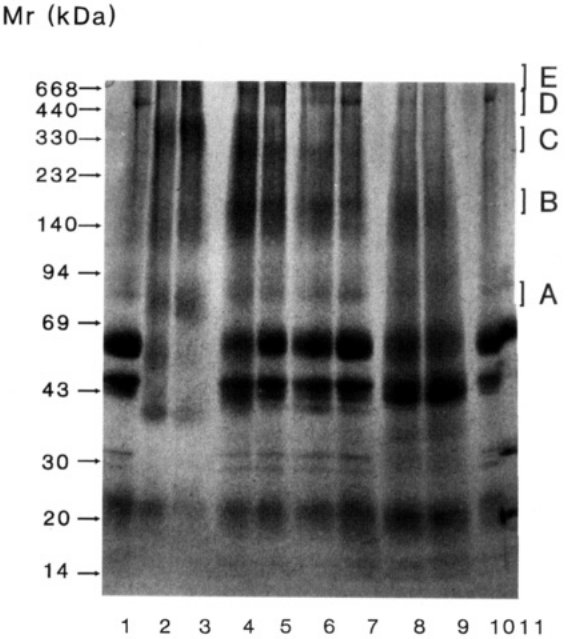

FIGURE 2: SDS−polyacrylamide gel electrophoresis of the cross-linked GAL−CathA complex. Lanes 1 and 10 represent the native complex under nonreducing conditions, and lane 11 represents the native complex under reducing conditions. The remaining lanes contain the complex cross-linked with 3,3′-DSP (0.1 and 0.2 mg/mL in lanes 2 and 3, respectively), DMS (2 and 1 mg/mL in lanes 4 and 5), DMA (2 and 1 mg/mL in lanes 6 and 7), and EDC (1 and 2 mg/mL in lanes 8 and 9). The arrows at the left indicate the position of the low and high molecular weight markers; the clamps at the right indicate the cross-linked species further used in the cleavage analysis. A 5−15% (w/v) gradient polyacrylamide gel was used. Proteins were stained by Coomassie blue R-250.

dissociated by overnight incubation at pH 7.5 prior to the cross-linking. The higher electrophoretic mobility of the GAL (apparent molecular mass of 58 instead of 64 kDa) and CathA (40 instead of 49 kDa) monomers on the SDS gel after treatment of the complex with 3,3′-DSP is probably due to the formation of internal disulfide bridges in these monomers. The same phenomenon of internal cross-linking

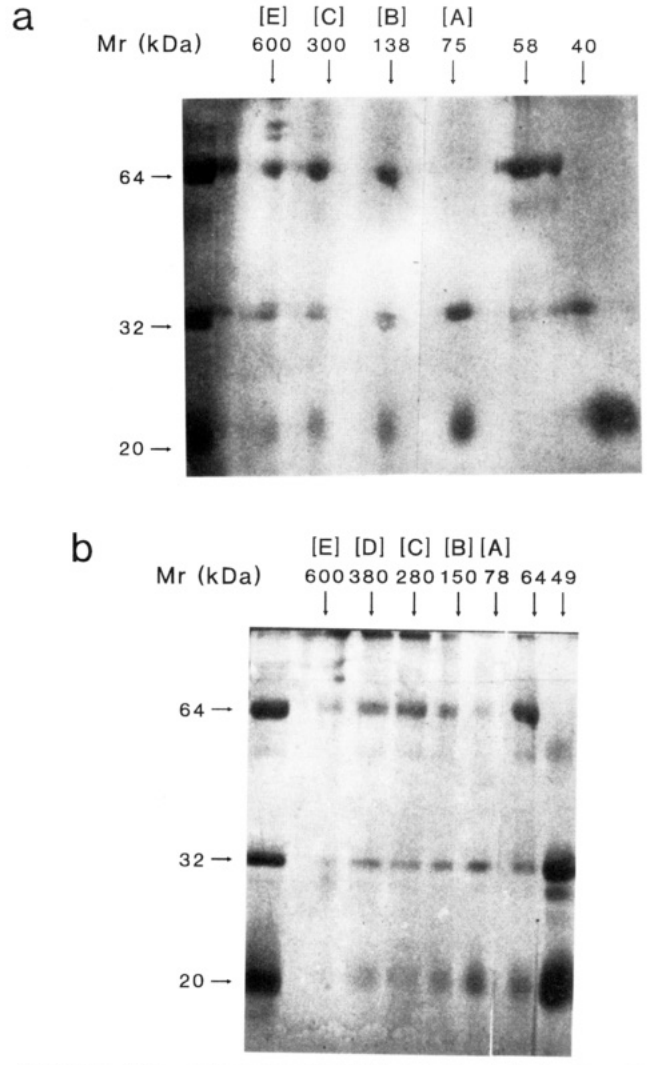

FIGURE 3: SDS−polyacrylamide [11% (w/v)] gel electrophoresis of protomers obtained by cleavage of cross-linked products of the GAL−CathA complex. The complex was cross-linked by 3,3′-DSP (a) and DMS (b), and the products were separated by the first SDS−PAGE as described in Figure 2. The Coomassie blue-stained bands of cross-linked products were excised from the gel and transferred to the appropriate reaction medium to cleave the cross-linkers: 2% (w/v) DTT and 0.2% (w/v) SDS in 0.75 M Tris-HCl buffer, pH 6.8 for 3,3′-DSP and a mixture of 40% (v/v) methylamine solution, concentrated HCl, and acetonitrile (7:1:24 v/v/v) for DMS. After the second electrophoresis the gels were stained by combined Coomassie blue R-250 and silver staining. The left lanes on both panels contained the noncross-linked complex as markers for the position of GAL and CathA protomers. The cross-linked products (refer to Figure 2 and Table 2) and their molecular masses in the first gel are indicated at the top of each panel.

is likely responsible for the appearance of double CathA bands after treatment with DMS and DMA (Figure 2).

To analyze the composition of the cross-linked species separated by SDS−PAGE, the protein bands were excised from the stained gel, soaked in an appropriate reagent to cleave the cross-linked products, and analyzed by a second SDS−PAGE. In this second gel (Figure 3), the rate of migration of the cleavage products was directly compared with that of GAL and CathA protomers. The molar ratio of GAL to CathA in each cross-linked product was measured by microdensitometric analysis of the stained gels. The results of the analysis (Figure 3 and Table 2) indicate that the 70−80-kDa products [A] cross-linked by both 3,3′-DSP and DMS represent the CathA dimer. All other products

Table 2: Composition of the Main Cross-Linked Products of the GAL−CathA Complex[a]

cross-linker	band on gel[b]	M_r (kDa)	GAL:CathA (molar ratio)	deduced protomer composition
3,3′-DSP	[A]	75 ± 20	1:28	$(CathA)_2$
	[B]	138 ± 15	1:1.65	$GAL(CathA)_2$
	[C]	300 ± 20	1:2.1	$GAL_2(CathA)_4$
	[E]	550−600	1:1.9	$GAL_4(CathA)_8$
DMS	[A]	78 ± 20	1:14.3	$(CathA)_2$
	[B]	150 ± 10	1:1.8	$GAL(CathA)_2$
	[C]	280 ± 20	1:1.8	$GAL_2(CathA)_4$
	[D]	380 ± 20	1:1.9	$GAL_3(CathA)_6$
	[E]	550−600	1:1.7	$GAL_4(CathA)_8$

[a] The products, separated by gradient SDS−PAGE, were cleaved by treatment with DTT or methylamine and analyzed by a second SDS−PAGE as described in Experimental Procedures. The GAL:CathA molar ratio was measured by microdensitometric analysis. [b] See Figure 2 for corresponding bands.

cross-linked with 3,3′-DSP or DMS (Table 2) contain both GAL and CathA monomers in an approximately 1:2 molar ratio as previously reported for the complex itself (Pshezhetsky & Potier, 1993). Cross-linked species are identified from their monomer composition as $GAL(CathA)_2$ for [B], $(GAL)_2(CathA)_4$ for [C], $(GAL)_3(CathA)_6$ for [D], and $(GAL)_4(CathA)_8$ heterooligomers for [E], respectively (Table 2). The small differences in molecular masses between the same products cross-linked by 3,3′-DSP and DMS are probably due to the formation of internal disulfide bridges in GAL and CathA monomers after treatment with 3,3′-DSP as discussed above. Thus, on the basis of both radiation inactivation and cross-linking experiments, the $GAL(CathA)_2$ heterotrimer (168 kDa) is proposed as the basic subunit of the 680-kDa GAL−CathA complex which would be formed by the association of four such subunits.

Selection of CathA-Derived Peptides. The surface of the CathA dimer quaternary structure model (Elsliger & Potier, 1994) was analyzed for a possible GAL-binding interface. The solvent accessibility of the amino acid residues in the CathA dimer structure was used as the initial criteria for the selection of peptide segments that could potentially interact with GAL. Residue side chains with surface accessibilities greater than 30 Å^2 were classified as solvent accessible. Initially, 13 peptide segments were selected (filled bars in Figure 4). Visualization of these segments on the model of the CathA dimer structure (Figure 5) allowed us to exclude 8 of them on the basis of their proximity to the active site (peptides V, VI, XI, and XII), N-glycosylation sites (I, IV, and X), or dimer interface (VII and XII), which would physically hamper any interaction with another protein. Finally, we selected two (peptides III and XIII) of the five remaining segments because they are located at the ridge of a cavity formed by the dimerization of CathA monomers (Figure 5), which is large enough to accommodate a 64-kDa GAL monomer with a Stokes radius of about 28 Å (Pshezhetsky et al., 1992). The computed solvent-accessible surface of this cavity is 3500 Å^2, which should cover about 35% of the total theoretical surface of GAL calculated from the equivalent sphere (9852 Å^2). Synthetic peptides corresponding to segments III and XIII were named PC-2 and PC-1, respectively. A third synthetic peptide, PC-3, corresponding to segment VIII located on the opposite side of the CathA structure (Figure 5), was used as a control peptide

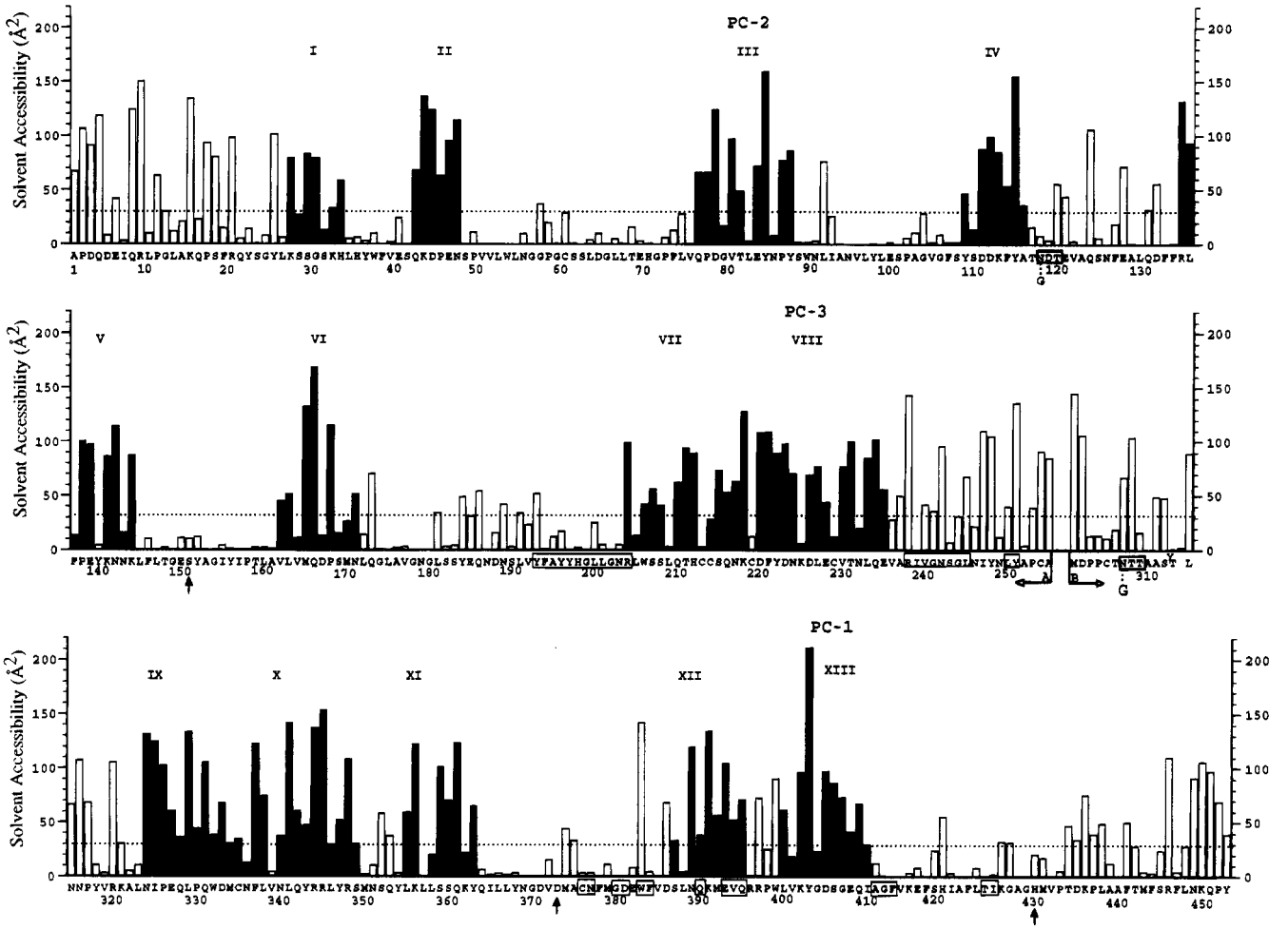

FIGURE 4: Solvent accessibility (Å^2) of amino acid residues of CathA. Candidate peptide segments, which correspond to our criteria for possible interaction with GAL (30 Å^2 cutoff, presented as a dotted line), are numbered from I to XIII and filled in black. The active site triad residues (Ser^{150}, Asp^{372}, and His^{429}) are indicated by an arrow. Dimer interface residues are boxed, and glycosylation sites are boxed with an attached G.

in complex dissociation and reconstitution experiments. As an unrelated control peptide angiotensin II was used.

Reconstitution of the GAL−CathA Complex in the Presence of CathA-Derived Peptides. We have previously reported that the 680-kDa GAL−CathA complex can be reconstituted *in vitro* by mixing the purified GAL and CathA in a 1:2 molar ratio at pH 4.75 (Pshezhetsky & Potier, 1993). Here we used this system to study the interaction of the CathA-derived synthetic peptides with GAL. The results show that approximately the same amount of reconstituted complex was formed in the absence of peptides or in the presence of human angiotensin II and PC-3 (Table 3). In contrast, both PC-1 and PC-2 were found to inhibit the reconstitution of the GAL−CathA complex (Table 3).

Dissociation of the GAL−CathA Complex by CathA-Derived Peptides. CathA-derived peptides were also tested for their capacity to dissociate the complex. Since the complex is in a dynamic equilibrium with its components (Pshezhetsky & Potier, 1993), peptides with high affinity for GAL will push the equilibrium toward complex dissociation. As shown in Table 4, in concentrated preparations of the GAL−CathA 680-kDa complex, the equilibrium is completely shifted toward the GAL−CathA complex formation with only about 4% of GAL and 1% of CathA being in a free form. This ratio was not changed in the presence of 10 mM PC-3. However, incubation of the GAL−CathA complex with 10 mM PC-1 or with 10 mM PC-2 (Table 4) for 1 h resulted in an about 30% dissociation of the complex. The same 30% dissociation was obtained in the presence of both PC-1 and PC-2 (1:1 molar ratio) but in a much lower concentration (2 mM). At 10 mM concentration, combined PC-1 and PC-2 resulted in about 90% dissociation of the complex (Table 4).

PC-1 Binding to GAL and the GAL−CathA Complex. To demonstrate the direct binding of PC-1 to GAL and the GAL−CathA complex, we incubated the purified complex with increasing concentrations of ^{125}I-labeled PC-1. The FPLC gel filtration analysis of the preparation (Figure 6) shows that the radioactivity peaks coeluted with the protein peaks corresponding to the GAL−CathA complex and GAL tetramers. As expected, no radioactivity coeluted with the CathA dimer, indicating that PC-1 binds specifically to GAL. The determination of the binding constant using a Scatchard plot yielded the same K_d of 1.3 ± 0.1 mM for both the GAL−CathA complex and individual GAL tetramers whereas the n value was 1.52 ± 0.2 for GAL and 0.97 ± 0.1 for the GAL−CathA complex. This result suggests that the binding of two PC-1 molecules to one GAL monomer is required for complex dissociation.

Effect of PC-1 on the Kinetic Parameters of GAL. In agreement with direct binding to GAL, PC-1 was found to influence the kinetic parameters of the free GAL tetramer.

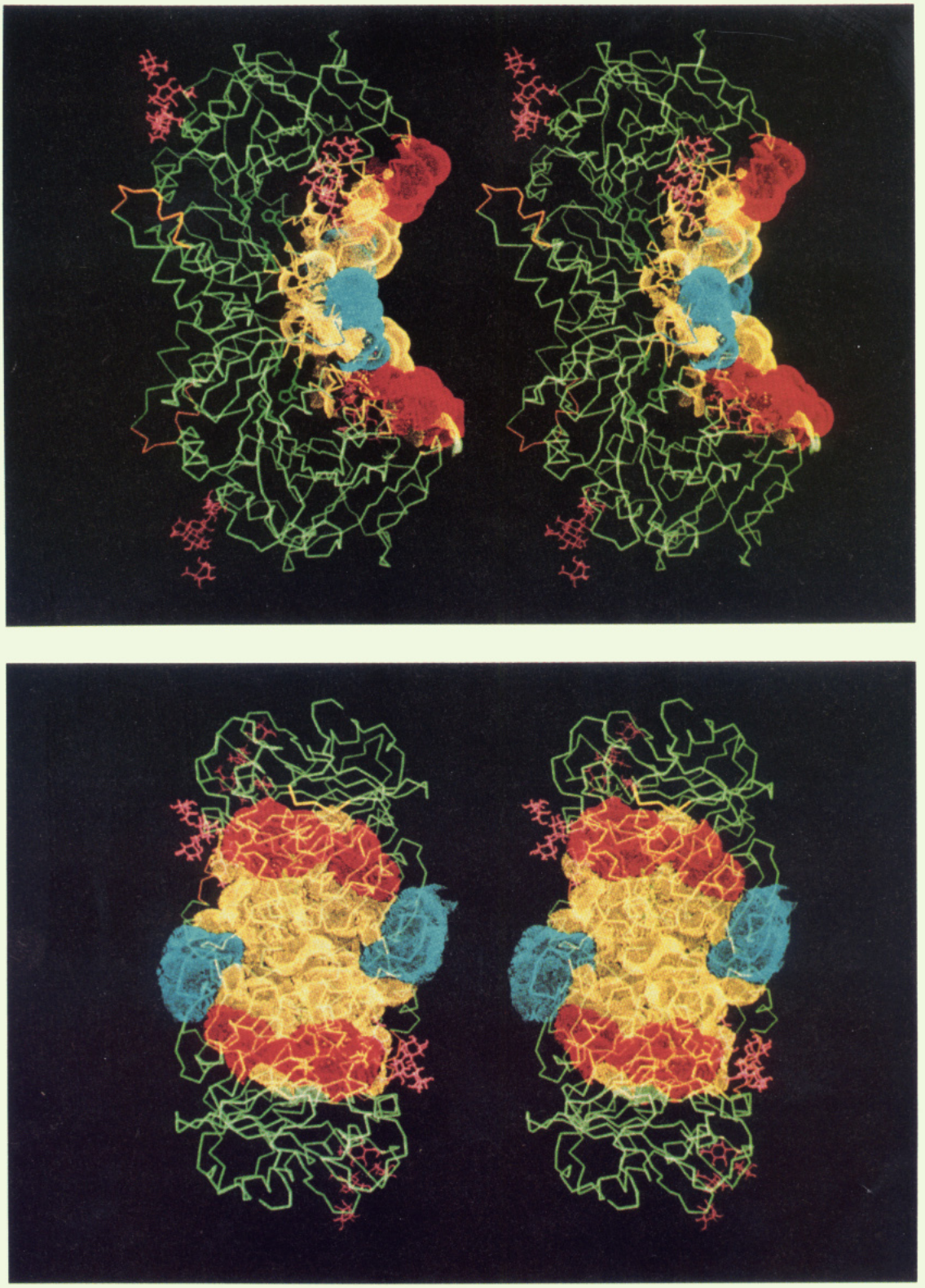

FIGURE 5: Stereo side (top) and front (bottom) views of the C_α trace of the CathA dimer. The location of the proposed GAL-binding interface is indicated by a solvent-accessible dot surface. The synthetic peptide PC-1 is indicated in red surface and PC-2 in blue surface. PC-3 is indicated as an orange trace. Glycosylation sites are indicated in pink and the active site triad residues Ser^{150}, Asp^{372}, and His^{429} in dark green.

Incubation of GAL preparations with PC-1 increased the initial rate of Muf-β-GAL hydrolysis (Figure 7) with an activation constant, K_a, of 0.78 ± 0.13 mM, which is similar to the K_d value of 1.3 ± 0.1 mM found for this peptide (Figure 6). The analysis of substrate dependencies of the initial reaction rate in the presence and in absence of PC-1 (Figure 7, inset) indicated that the peptide lowered the K_m from 0.62 to 0.27 mM but did not change the k_{cat} of the reaction. The same effect on GAL tetramers was also observed with the addition of the CathA dimer instead of PC-1, but with a K_a of 0.35 ± 0.15 μM (data not shown). In a saturating concentration of PC-1 (10 mM) no further activation of GAL by CathA was observed. Neither PC-1 nor CathA were able to activate GAL in the GAL−CathA

Table 3: Effect of CathA-Derived Synthetic Peptides on the Reassociation of GAL and CathA[a]

peptide	concn (mM)	% of reconstituted GAL−CathA complex (% of control)[b]
no addition	0	100 ± 15
angiotensin II	10	107 ± 12
PC-1	2	73 ± 23
	10	11 ± 6
PC-2	10	25 ± 8
PC-3	10	106 ± 22
	20	70 ± 18

[a] Individual GAL and CathA preparations (both in buffer B, 0.25 mg/mL), at the indicated peptide concentration were mixed in a 1:2 molar ratio, incubated at 37 °C for 1 h, and analyzed by FPLC gel filtration to determine the proportion of the complex, free GAL, and free CathA. The amount of the GAL−CathA complex formed is presented as the percent of the control without added peptide. [b] The data represent the average value of four different experiments ± SE.

Table 4: Effect of CathA-Derived Synthetic Peptides on the Dissociation of GAL−CathA Complex[a]

peptide	concn (mM)	% of free enzyme activity	
		CathA	GAL
no addition	0	0.8	3.8
PC-1	2.0	8.1	9.0
	10	30	28
PC-2	10	25	25
PC-3	2.0	1.2	4.0
	10	4.2	7
1:1 mixture of PC-1 and PC-2	1.0[b]	9.6	21
	2.0[b]	28	30
	5.0[b]	86	73
	10[b]	90	78

[a] Concentrated preparations of the GAL−CathA complex (0.8 mg of protein/mL) were diluted 1:2 in buffer A containing increasing concentrations of peptides and incubated at 36 °C for 60 min. The samples were then analyzed by FPLC gel filtration to determine the proportion of the complex, free GAL, and free CathA. [b] The indicated concentration is for each peptide.

680-kDa complex. Although the molecular mechanism and the biological role of this kinetic effect of CathA or CathA-derived peptides on GAL are not known, this result provides further evidence of specific PC-1 binding to GAL.

DISCUSSION

Previous studies on the *in vitro* dissociation and reconstitution of the 680-kDa GAL−CathA complex (Pshezhetsky & Potier, 1993; Ashmarina et al., 1994) indicated that it is composed of four GAL and eight CathA protomers and exists in dynamic equilibrium with free GAL tetramers and CathA dimers. These oligomers have been proposed as the basic structural elements of the complex. However, the present data on radiation inactivation analysis indicate that, in the complex, GAL and CathA propably adopt a different structure than that in their isolated oligomers, being in a 168-kDa subunit containing one GAL monomer and one CathA dimer. The destructive energy absorbed after a hit by an ionizing radiation seems to propagate inside this subunit, causing the simultaneous inactivation of both GAL and CathA. Indeed, the existence of such a subunit in the complex was further confirmed by chemical cross-linking experiments since all cross-linked products (Table 2) were formed by the association of the same basic 168-kDa GAL-$(CathA)_2$ subunit (up to four such subunits). The fact that

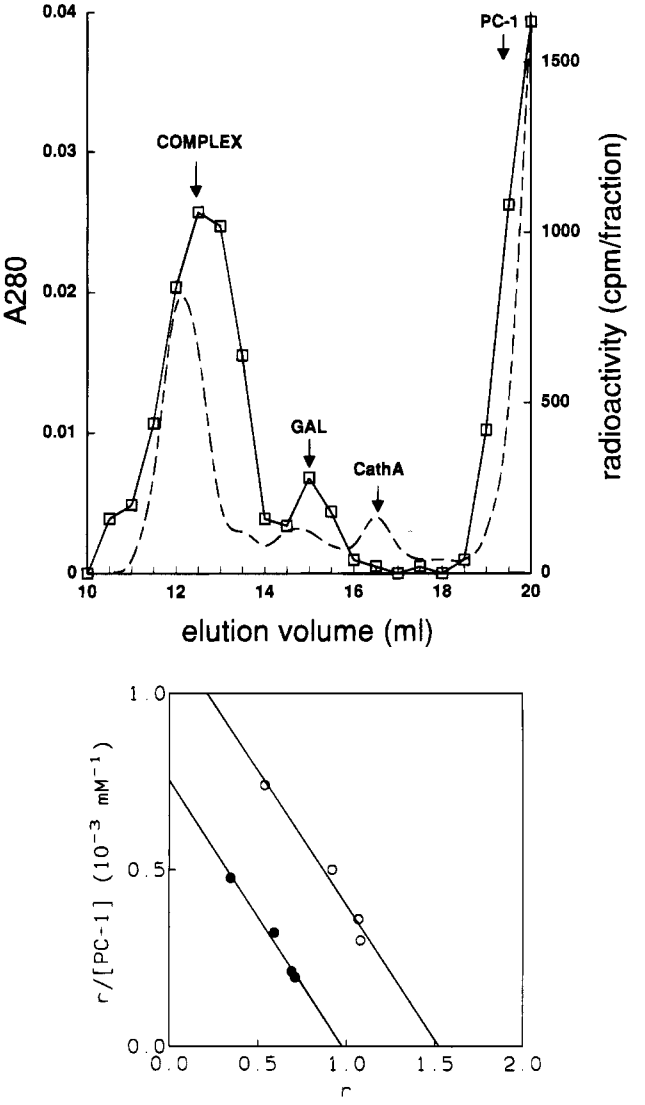

FIGURE 6: Superose 6 HR gel filtration of the GAL−CathA 680-kDa complex incubated for 1 h at 37 °C in the presence of 3.25 mM ^{125}I-labeled PC-1. Curves: (- - -) absorbance at 280 nm; (□) radioactivity (cpm/fraction). Conditions: column eluent, 20 mM sodium acetate buffer, pH 4.75, 0.15 M NaCl, 0.02% (w/v) NaN_3 (buffer A); sample volume, 50 μL (0.4 mg of protein/mL); flow rate, 0.4 mL/min. Fraction volume, 0.5 mL. Inset: Scatchard plot of radioactivity, incorporated into the GAL tetramers (○) or the GAL−CathA complex (●) on the concentration of ^{125}I -labeled PC-1 in the incubation media.

GAL−CathA complex dissociates *in vitro* into GAL tetramers and CathA dimers (Pshezhetsky & Potier, 1993) suggests that the 168-kDa subunit is not thermodynamically stable unless in the complex and its formation may require a conformational change in GAL or/and CathA. Evidence for such conformational change in GAL was also provided by the 2-fold reduction of the apparent K_m of GAL in the presence of CathA or CathA-derived PC-1.

The finding that the complex consists of four subunits each containing one GAL monomer associated with one CathA dimer inspired us to use the CathA dimer model to define a putative region of CathA involved in GAL binding. We assumed that synthetic peptides, corresponding to segments of the GAL-binding interface on CathA, should mimic the binding to complementary sites on GAL. Such peptides were chosen and experimentally tested for their effect on GAL−CathA complex reconstitution and dissociation. A similar

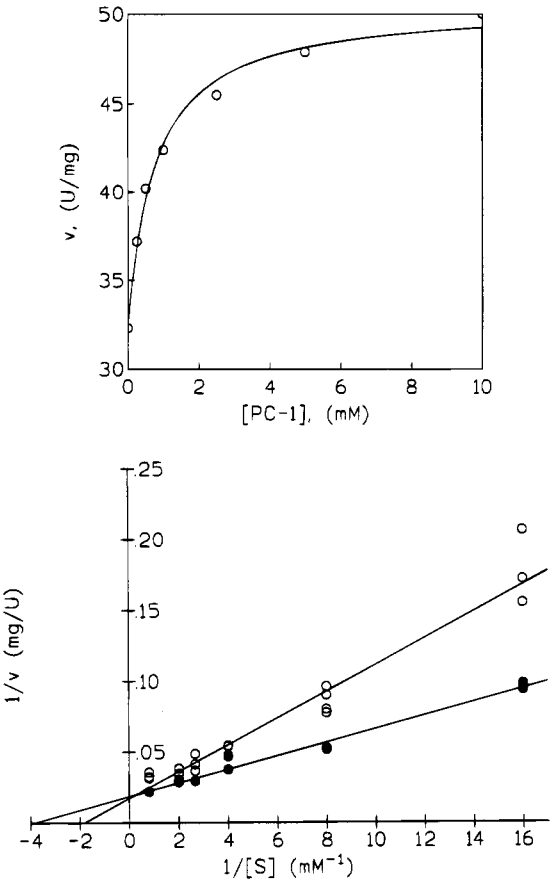

FIGURE 7: Activation of isolated GAL by PC-1. GAL was preincubated in buffer A, at 37 °C for 5 min in the presence of increasing concentrations of the PC-1 (0−10 mM) before the steady-state rate of Muf-β-GAL hydrolysis was measured at 0.0625 mM substrate concentration. Inset: Lineweaver−Burk plot of the substrate dependence of the initial rate of Muf-β-GAL hydrolysis catalyzed by GAL in the absence (○) or in the presence (●) of 10 mM PC-1.

approach has been successfully used to inhibit monomer−monomer interactions in troponin C (Blechner et al., 1992), ribonucleotide reductase from herpes simplex virus (Cohen et al., 1986; Dutia et al., 1986; Paradis et al., 1988; McClements et al., 1988), HIV-1 protease (Zhang et al., 1991), and reverse transcriptase (Divita et al., 1994).

Two CathA-derived synthetic peptides, PC-1 and PC-2, were found to hamper the formation of the GAL−CathA complex in both dissociation and reconstitution experiments (Tables 3 and 4). These results are consistent with the suggestion that both PC-1 and PC-2 bind to GAL, thus preventing its association with CathA. Indeed, the direct determination of the number of binding sites by Scatchard analysis with ^{125}I-labeled PC-1 revealed a stoichiometry of two peptide molecules per GAL monomer (Figure 6), which is in agreement with the 2:1 stoichiometry of CathA:GAL monomers in the complex (Pshezhetsky & Potier, 1993). One more evidence of PC-1 binding to GAL is provided by its effect on GAL kinetic parameters (Figure 7). Both CathA dimers and PC-1 activated GAL with the same magnitude although the activation constant for PC-1 was much higher. This could be predicted since PC-1 represents only a small part of the proposed GAL-binding interface on CathA. This is further supported by the much stronger effect of combined PC-1 and PC-2 on complex dissociation than of each peptide alone as expected if both PC-1 and PC-2 are involved in the GAL−CathA-binding interface. PC-3, the control peptide with physicochemical properties and amino acid composition similar to those of PC-1 and PC-2 had no influence on the dissociation or reconstitution of the complex. Since the p*I* values of all peptides are in the acidic range, unspecific electrostatic interactions with proteins should be minimized at the acidic pH used in all experiments. Altogether, these observations support the conclusion that interactions of PC-1 and PC-2 with GAL are specific and suggest that GAL binds to CathA dimer in a cavity formed by the association of the two monomers (Figure 5).

When the tertiary structure of human lysosomal GAL will be available, the same strategy can be used to define a contact region for CathA on the GAL molecule and to provide a more detailed model of the GAL−CathA complex. However, the present data on the localization of GAL monomers in the complex with 35% of their surface covered by the CathA dimer may explain the stabilizing effect of CathA on GAL in the lysosome, taking into account that CathA dimers are resistant to intralysosomal proteolytic digestion (Pshezhetsky & Potier, 1994).

NOTE ADDED IN PROOF

The crystallographic structure of CPDY has been published (Endrizzi et al., 1994) since the submission of this paper.

ACKNOWLEDGMENT

The authors are grateful to Drs. W. Kabsch and C. Sander for providing the DSSP program for solvent accessibility calculations, to Dr. S. J. Remington for providing the atomic coordinates of wheat carboxypeptidase II dimer and of yeast carboxypeptidase Y before publication, and to Dr. L. I. Ashmarina for critical reading of the manuscript.

REFERENCES

Ashmarina, L. I., Pshezhetsky, A. V., Spivey, H. O., & Potier, M. (1994) *Anal. Biochem. 219*, 349−355.
Beauregard, G., Maret, A., Salvayre, R., & Potier, M. (1987) *Methods Biochem. Anal. 32*, 313−343.
Blechner, S. L., Olah, G. A., Strynadka, N. C. J., Hodges, R. S., & Trewhella, J. (1992) *Biochemistry 31*, 11326−11334.
Bradford, M. M. (1976) *Anal. Biochem. 72*, 248−254.
Bragg, P. D., & Hou, C. (1986) *Arch. Biochem. Biophys. 244*, 361−373
Cohen, E. A., Gaudreau, P., Brazeau, P., & Langelier, Y. (1986) *Nature 321*, 441−443.
Connolly, M. L. (1983) *Science 221*, 709−713.
d'Azzo, A., Hoogeveen, A., Reuser, A. J., Robinson, D., & Galjaard, H. (1982) *Proc. Natl. Acad. Sci. U.S.A. 79*, 4535−4539.
Divita, G., Restle, T., Goody, R. S., Chermann, J.-C., & Baillon, J. G. (1994) *J. Biol. Chem. 269*, 13080−13083.
Dutia, B. M., Frame, M. C., Subak-Sharpe, J. H., Clark, W. N., & Marsden, H. S. (1986) *Nature 321*, 439−441.
Elsliger, M.-A., & Potier, M. (1994) *Proteins 18*, 81−93.
Endrizzi, J. A., Breddam, K., & Remington, S. J. (1994) *Biochemistry 33*, 11106−11120.
Galjart, N. J., Gillemans, N., Harris, A., van der Horst, G. T. J., Verheijen, F. W., Galjaard, H., & d'Azzo, A. (1988) *Cell 54*, 755−764.
Galjart, N. J., Morreau, H., Willemsen, R., Gillemans, N., Bonten, E., & d'Azzo, A. (1991) *J. Biol. Chem. 266*, 14754−14752.
Hoogeveen, A. T., Verheijen, F. W., & Galjaard, H. (1983) *J. Biol. Chem. 258*, 12143−12146.
Kabsch, W., & Sander, C. (1983) *Biopolymers 22*, 2577−2637.
Kempner, E. S., & Fleisher, S. (1989) *Methods Enzymol. 172*, 410−439.

Koenig, H. (1962) *Nature 195*, 782−785.
Laemmli, U. K. (1970) *Nature 227*, 680−685.
Lea, D. E. (1955) *Actions of Radiations on Living Cells*, 2nd ed., pp 69−99, Cambridge University Press, Cambridge.
Liao, D. I., Breddam, K., Sweet, R. M., Bullock, T., & Remington, S. J. (1992) *Biochemistry 31*, 9796−9812.
McClements, W., Yamanaka, G., Garsky, V., Perry, H., Baccheti, S., Colonno, R., & Stein, R. B. (1988) *Virology 162*, 270−273.
Morreau, H., Galjart, N. J., Willemsen, R., Gillemans, N., Zhou X. Y., & d'Azzo, A. (1992) *J. Biol. Chem. 267*, 17949−17956.
Okada, S., & O'Brien, J. S. (1968) *Science 160*, 1002−1004.
Palmeri, S., Hoogeveen, A. T., Verheijen, F. W., & Galjaard, H. *(1986) Am. J. Hum. Genet. 38*, 137−148.
Paradis, H., Gaudreau, P., Brazeau, P., & Langelier, Y. (1988) *J. Biol. Chem. 263*, 16045−16050.
Potier, M., Thauvette, L., Michaud, L., Giroux, S., & Beauregard, G. (1991) *Biochemistry 30*, 8151−8157.
Potier, M., Villemure, J.-F., & Thauvette, L. (1994) *Biochem. J. 298*, 571−574
Pshezhetsky, A. V., & Potier, M. (1993) *Biochem. Biophys. Res. Commun. 195*, 354−362.
Pshezhetsky, A. V., & Potier, M. (1994) *Arch. Biochem. Biophys. 313*, 64−70.
Pshezhetsky, A. V., Levashov, A. V., & Wiederschain, G. Ya. (1992) *Biochim. Biophys. Acta 1122*, 154−160.
Scatchard, G. (1949) *Ann. N.Y. Acad. Sci. 51*, 660−662.
Shimmoto, M., Fukuda, Y., Itoh, K., Oshima, A., Sakuraba, H., & Suzuki, Y. (1993) *J. Clin. Invest. 91*, 2393−2399.
Suzuki, Y., Sakuraba, H., Yamanaka, T., Ko, Y. M., Iimori, Y., Okamura, Y., & Hoogeveen, A. T. (1984) in *The Developing Brain and Its Disorders* (Arina, M., Suzuki, Y., & Yabuuchi, H., Eds) pp 161−175, University of Tokyo Press, Tokyo.
Tranchemontagne, J., Michaud, L., & Potier, M. (1990) *Biochem. Biophys. Res. Commun. 168*, 22−29.
Van der Horst, G. J., Galjart, N. J., d'Azzo, A., Galjaard, H., & Verheijen, F. W. (1989) *J. Biol. Chem. 264*, 1317−1322.
Verheijen, F. W., Palmeri, S., Hoogeveen, A. T., & Galjaard, H. (1985) *Eur. J. Biochem. 149*, 315−321.
Wenger, D. A., Tarby, T. J., & Wharton, C. (1978) *Biochem. Biophys. Res. Commun. 82*, 589−595.
Zhang, Z. Y., Poorman, R. A., Maggiora, L. L., Heinrikson, R. L., & Kézdy, F. J. (1991) *J. Biol. Chem. 266*, 15591−15594.
Zhou, X. Z., Galjart, N. J., Willemsen, R., Gillemans, N., Galjaard, H., & d'Azzo, A. (1991) *EMBO J. 10*, 4041−4048.

BI942230U